5 Surface/Interface Project – Crystalline, magnetic and electronic structures at the surface and interface of magnetic thin films and multilayers –

Project Leader: Kenta Amemiya

5-1 Introduction

The surface and interface of magnetic thin films play essential roles in the appearance of extraordinary magnetic properties such as perpendicular magnetic anisotropy (PMA) and the giant magnetoresistance effect. We are investigating the crystalline, magnetic and electronic structures at the surface and interface of magnetic thin films and multilayers, in order to reveal the origin of fascinating magnetic properties that cannot be realized in bulk materials. For example, we have studied magnetic anisotropy of Fe/Ni multilayers [1-3], magnetic structures at the interface between antiferromagnetic FeMn and ferromagnetic Ni, effects of ion irradiation on ultrathin films [4,5], and magnetic depth profile of Gd/Cr multilayers, by means of X-ray magnetic circular dichroism (XMCD) and polarized neutron reflectivity techniques. We also plan to perform muon spin rotation experiments using an ultra-slow muon source.

5-2 Scientific topics: Control of magnetic anisotropy of Fe/Ni multilayers through lattice distortion [1-3]

The $L1_0$-type Fe/Ni multilayer has attracted much attention as a candidate material for rare metal-free perpendicularly magnetized films for high-density recording media. The $L1_0$ ordered structure consists of alternate stacking of two different atomic planes along the fcc [001] direction as illustrated in Fig. 1, and is expected to exhibit uniaxial magnetic anisotropy in the c axis, [001]. Therefore, efforts have been made to realize PMA by using alternate monatomic layer deposition on fcc (001) substrates [6-8]. Our recent in-situ XMCD study revealed element-specific magnetic anisotropy energies (MAEs) in Fe/Ni ultrathin films on Cu(001) substrate [1], but the result was based on the assumption that the structure of the film is uniform regardless of the film thickness. To understand the magnetic anisotropy of magnetic multilayers correctly, it is necessary to consider the effects of structural changes because the lattice constant of actual systems may differ from those of ultrathin films. The MAE of alloy materials such as Fe/Ni multilayer, in which the magnetic moment is carried by different magnetic elements, should be analyzed element-specifically. In addition, to separately obtain the signals from the surface and buried layers, depth-resolved analysis is also necessary. In the present study, we applied in-situ reflection high energy electron diffraction (RHEED) and depth-resolved XMCD analyses to alternately layered FeNi ultrathin films grown on Ni(3–21 ML)/Cu(001).

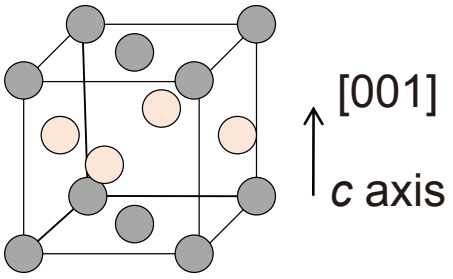

Fig. 1: Schematic illustration of the $L1_0$ structure.

The 1 ML Fe and 1 ML Ni layers were alternately grown on a wedge-shaped Ni(3–21 ML)/Cu(001) substrate. All the samples showed almost the same RHEED pattern, which suggests that Fe and Ni grow epitaxially on the Cu(001) substrate. The Ni/Cu(001) system has a relatively small lattice mismatch of 2.6%, and is known to grow pseudomorphically on Cu(001) up to ~13 ML, from which the film begins to relax as misfit dislocation forms. On the other hand, since Ni/Cu(001) shows the spin reorientation transition (SRT) from in-plane to perpendicular directions at a thickness between 7 and 11 ML, both perpendicular and in-plane magnetized FeNi films on Ni(3–21 ML)/Cu(001) can be obtained. Therefore, both the structure and magnetic anisotropy of the FeNi film are expected to be controllable when the wedge-shaped Ni(3–21 ML)/Cu(001) is used as the substrate.

The in-plane lattice constant, *a*, of FeNi and Ni films was estimated from the RHEED pattern, by using that for the Cu(001) substrate, whose lattice constant is 0.255 nm, as a reference. In the present study, the nearest in-plane interatomic distance is referred to as the in-plane lattice constant, *a*. Figure 2 shows *a* as a function of total film thickness, $n + x$, for FeNi(*n* ML)/Ni(*x* ML)/Cu(001). The FeNi films grow with similar *a* to that of Cu up to the total film thickness, $n + x$, of ~ 13 ML, after which the decrease in *a* occurs. The slope of the decrease in *a* of FeNi is larger than that of Ni. This might be interpreted as being due to the fact that the surface tension of Fe is larger than that of Ni, and Fe would partly take a discontinuous structure in the in-plane direction approaching its own lattice constant,

which leads to the rapid relaxation of the lattice. Therefore, we assume that the growth process is divided into two regions, in which *a* is expressed as the solid line in Fig. 2.

First, we estimate the MAE of Fe layers sandwiched by Ni layers. We use 4 and 6 ML FeNi films to obtain the signal from the Ni-sandwiched Fe layers. Figure 3 shows Fe L-edge XMCD spectra for a 4 ML FeNi film grown on Ni(*x* ML)/Cu(001) taken in the total electron yield mode. The films show in-plane and perpendicular magnetization at x = 8 and 21 ML, respectively. Since the in-plane lattice constant, a, can be estimated from Fig. 2, we obtain $m_l^{\perp}/m_s^{\mathrm{eff}}$(Fe) = 0.20(3) at a = 0.248 nm (x = 21) and $m_l^{//}/m_s^{\mathrm{eff}}$(Fe) = 0.15(3) at a = 0.253 nm (x = 8), where m_s^{eff}(Fe) represents the effective spin magnetic moment of Fe. m_s^{eff}(Fe) was estimated from sum-rule analysis [9,10]. Similarly, $m_l^{\perp}/m_s^{\mathrm{eff}}$(Fe) and $m_l^{//}/m_s^{\mathrm{eff}}$(Fe) are estimated as functions of a from a set of data at different x and n.

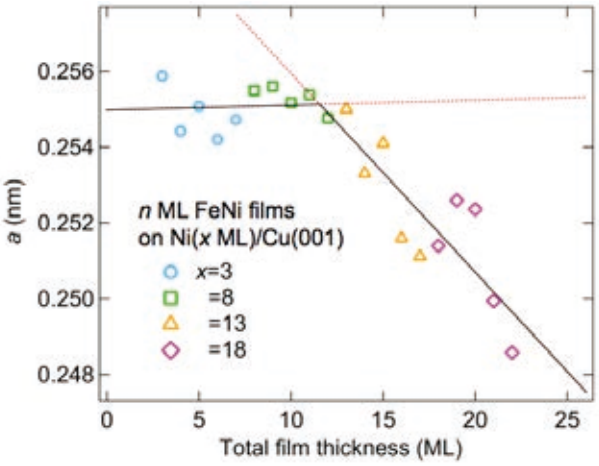

Fig. 2: In-plane lattice constant, *a*, of *n* ML FeNi films on Ni(*x* ML)/Cu(001) as a function of total film thickness, *n* + *x*. *n* (= 0–4) ML FeNi films with four different *x* (= 3, 8, 13, and 18) are investigated.

Next, we estimate the MAE of Ni layers sandwiched by Fe layers. Because the Fe-sandwiched Ni layer should be distinguished from the substrate Ni layer for a quantitative estimation of MAE, we applied the depth-resolved XMCD technique [11,12] and extracted layer-resolved components of the XMCD spectra from a set of data with different probing depths, $_e$. In the extraction procedure, the Ni layers in FeNi(3 ML)/Ni(*x* ML)/Cu(001) are divided into three regions: the Fe-sandwiched Ni layer with a 1 ML thickness, the top 1 ML of substrate Ni, and the remaining Ni layers. In the case of FeNi(5 ML)/Ni(*x* ML)/Cu(001), the Ni layers are also divided into three regions, but two Fe-sandwiched Ni layers, the second and fourth layers from the surface, are assumed to have the same XMCD spectra. The

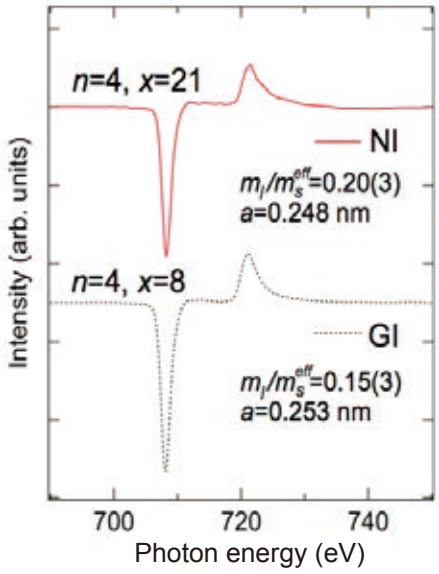

Fig. 3: Fe L-edge XMCD spectra for *n* ML FeNi films grown on Ni(*x* ML)/Cu(001) taken in the total electron yield mode. 4 ML FeNi films at x = 21 and 8 show perpendicular and in-plane magnetization, and the XMCD data were measured at normal (NI) and grazing (GI) incidence angle configurations, respectively.

XMCD spectra of these three regions are determined so as to reproduce the observed spectra with different $_e$ by the superposition of three components with proper spectral weights depending on $_e$. The extracted spectra of the Fe-sandwiched Ni layer are shown in Fig. 4. The obtained m/m_s^{eff}(Ni) is 0.07(2) and 0.10(3) for a 3 ML FeNi film at x = 20 and a 5 ML FeNi film at x = 8.3, respectively, where m_s^{eff}(Ni) represents the effective spin magnetic moment of Ni.

Figure 5 shows m/m_s^{eff} in the perpendicular and in-plane directions of sandwiched-Fe (a) and Ni (b) layers as a function of in-plane lattice constant, a. To avoid underestimating the spin and orbital magnetic moments, which sometimes occurs in the remanent state due to the domain formation, we fix m_s^{eff} at the value obtained from a magnetically saturated film. In the present study, we chose the 4 ML FeNi film at x = 10 and the 3 ML FeNi film at x = 16 for the analysis of the moment in Fe and Ni, respectively. In the sum-rule analysis, the d-hole numbers of Fe and Ni are assumed to be 3.0 and 1.5, and m_s^{eff} (Fe) = 1.6 μ_B and m_s^{eff} (Ni) = 0.73 μ_B are obtained. The d-hole number of the other sample is estimated based on the assumption that the white line intensity is proportional to the d-hole number. The white line intensity is obtained after subtracting the step function from the polarization-averaged X-ray absorption spectra. We find no significant change in the d-hole number for other samples, which suggests no or little difference in the electronic structure.

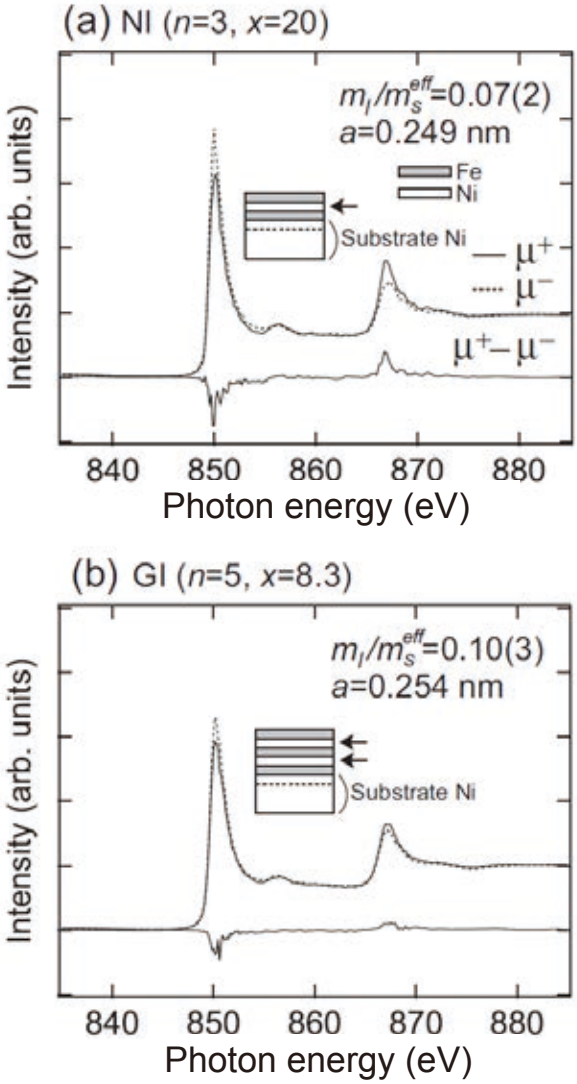

Fig. 4: Extracted Ni L-edge circularly polarized x-ray absorption (μ+ and μ−) and XMCD (μ+ − μ−) spectra for the Ni layer in *n* ML FeNi film grown on Ni (*x* ML)/Cu(001). 3 and 5ML FeNi films at *x* = 20 and 8.3 show perpendicular and in-plane magnetization, respectively. The models used in the extraction procedure are also illustrated.

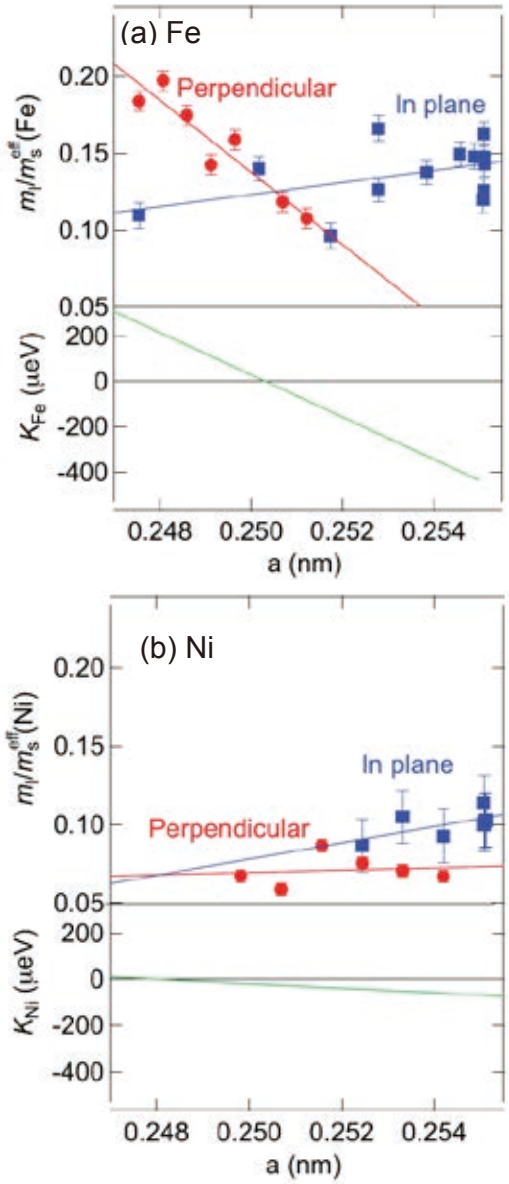

Fig. 5: Ratios of orbital magnetic moment to spin moment in the perpendicular (red circle) and in-plane (blue square) directions, and magnetic anisotropy energy of (a) Fe and (b) Ni layers as a function of in-plane lattice constant, *a*, estimated by using proportional factors, *F*, of 2.0 and 3.0 meV/μ_B for Fe and Ni, respectively.

For Ni-sandwiched Fe, the perpendicular component of the orbital magnetic moment, $m_l^{\perp}$, increases and the in-plane component, $m_l^{//}$, decreases as *a* gets smaller. This indicates that PMA is enhanced when the compressive strain in the in-plane direction is applied to the Fe layer. On the other hand, in the case of the Fe-sandwiched Ni layer, the orbital magnetic moment in both directions shows a small dependence on *a* within the error margins of ~0.02 μ_B. We then perform a linear fit to the data and estimate $m_l^{\perp}$ and *m*// and then MAE, assuming that the MAE is expressed as F ($m_l^{\perp}$ - $m_l^{//}$) [13], as functions of *a*. The MAE of Ni-sandwiched Fe, K_{Fe}, is plotted by using the reported *F* for Fe, 2.0 ± 0.8 meV/μ_B [14], as shown in Fig. 5(a).

Although the absolute value of the energy is not very reliable, the relative comparison against *a* can be relevant. The MAE in Fe strongly depends on the in-plane lattice constant, and it is necessary to make *a* smaller than 0.25 nm in order to realize positive MAE. On the other hand, the MAE in Ni is also obtained by using the reported *F* for Ni, 3.0 ± 0.5 meV/μ_B [13], which is shown in Fig. 5(b). The anisotropy of the orbital moment in Ni is not sensitive to the structural change, and the dependency of MAE on the structure is within the error margin of ~±40 μeV per atom. The difference

between Fe and Ni might be because the anisotropy of Fe orbitals near the Fermi level is more sensitive to the structural change than that of Ni. In fact, it is reported from first-principles calculations on $L1_0$-type FeNi that only Fe components of the orbital density of states exist at the Fermi level [15]. Moreover, recent theoretical work also reported that PMA of the $L1_0$-type FeNi arises predominantly from Fe atoms, and that compressive in-plane distortion can enhance PMA. This was explained as being due to the modulation of the Fe d(xy) and $d(x^2 - y^2)$ orbital components [16]. Although a detailed discussion on the electronic structures of Fe and Ni is not presented here, we emphasize that the compressive strain in Fe must be effective to realize PMA, e.g., by inserting a proper buffer layer.

5-3 Experimental technique: Polarized neutron reflectivity experiment at BL-17 in J-PARC

Polarized neutron reflectivity (PNR) is one of the most powerful techniques to investigate the magnetic depth profile of thin films and multilayers. Since PNR is sensitive to the buried interface, it is complementary to XMCD in the soft X-ray region, which is quite surface sensitive with a typical probing depth of a few nm. Recently, a PNR station, SHARAKU, has been developed at BL-17 in J-PARC (Fig. 6), and we performed a PNR experiment for a FeMn/Ni/Cu(001) film, in order to observe the canted component of magnetic moment in the ferromagnetic Ni film at the interface with the antiferromagnetic FeMn layer.

Fig. 6: Experimental setup for polarized neutron reflectivity at BL-17 in J-PARC.

Figure 7 shows preliminary data for Cu(100 ML)/FeMn(25 ML)/Ni(16 ML)/Cu(100), taken at room temperature. Since the overall magnetization of Ni film is almost perpendicular to the surface, only a small difference between opposite polarizations at 0.1 T is reasonable because PNR is sensitive to the in-plane magnetic component. In contrast, a significant signal is found at 1 T, indicating that magnetization of the film is forced to align in the in-plane direction. Further development is expected in order to investigate the interface magnetic structure of ultrathin films.

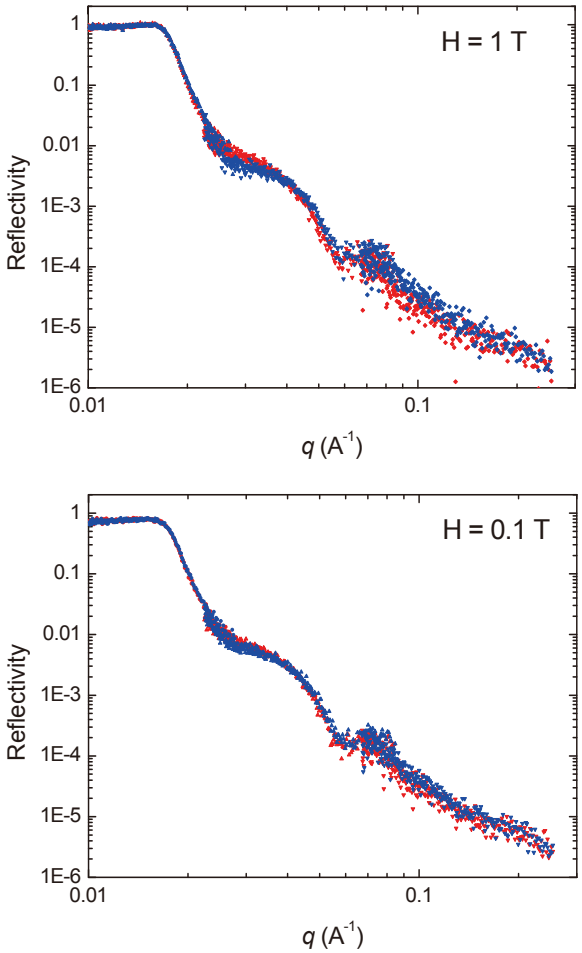

Fig. 7: Polarized neutron reflectivity curve for Cu(100 ML)/FeMn(25 ML)/Ni(16 ML)/Cu(001) taken at room temperature at 1 and 0.1 T.

References

[1] M. Sakamaki and K. Amemiya, Appl. Phys. Express **4** (2011) 073002.

[2] M. Sakamaki and K. Amemiya, e-J. Surf. Sci. Nanotech. **10** (2012) 97.

[3] M. Sakamaki and K. Amemiya, Phys. Rev. B **87** (2013) 014428.

[4] M. Sakamaki et al., Phys. Rev. B **86** (2012) 024418.

[5] K. Amemiya et al., Eur. Phys. J. Web of Conferences **40** (2013) 08002.

[6] T. Shima et al., J. Magn. Magn. Mater. **310** (2007) 2213.

[7] M. Mizuguchi, et al., J. Appl. Phys. **107** (2010) 09A716.

[8] T. Kojima et al., J. Phys.: Conf. Ser. **266** (2011) 012119.
[9] B. T. Thole, P. Carra, et al., Phys. Rev. Lett. **68** (1992) 1943.
[10] P. Carra, et al., Phys. Rev. Lett. **70** (1993) 694.
[11] K. Amemiya, Phys. Chem. Chem. Phys. **14** (2012) 10477.
[12] K. Amemiya et al., Appl. Phys. Lett. **84** (2004) 936.
[13] P. Bruno, Phys. Rev. B 39 (1989) R865.
[14] H. Abe et al., J. Magn. Magn. Mater. **302** (2006) 86.
[15] P. Ravindran et al., Phys. Rev. B **63** (2001) 144409.
[16] Y. Miura et al., J. Phys.: Condens. Matter **25** (2013) 106005.